J. Fluid Mech. (1967), *vol.* 29, *part* 1, *pp.* 81–92
Printed in Great Britain

Balance of turbulence energy in the region of jet-flow establishment

By SEDAT SAMI†
Institute of Hydraulic Research, The University of Iowa, Iowa City

(Received 18 August 1966 and in revised form 26 January 1967)

To complete a previous investigation reported earlier and carried out in an air jet issuing from a 1·0 ft. diameter nozzle into still air, additional measurements were made of one-point triple-velocity and two-point double-velocity correlations and the spatial mean gradients of the axial turbulent velocities. The one-point pressure/axial-velocity correlation term was evaluated by using piezo-electric ceramic elements in conjunction with total- and static-pressure probes. For the measurement of spatial mean gradients of the axial-velocity fluctuation, special probes with two parallel wires were constructed. The axial scale of turbulence was found to be almost twice as large as the other two scales. The tangential scale was the smallest. All terms of the integral and differential forms of the turbulence energy equation were evaluated throughout the region and the results are given in dimensionless form.

1. Introduction

In a previous study (Sami, Carmody & Rouse 1967) measurements leading to the evaluation of the velocity and pressure fields of a diffusing jet were reported in detail and the momentum and mean-energy equations were seen to be satisfied within satisfactory limits. The investigation has been brought to its natural conclusion by also studying the turbulence-energy equation. The measurement of all the terms involved in the equation and the balance of the equation itself are presented herein. In addition, the axial, radial and tangential scales of turbulence were investigated for the region of flow establishment.

2. Experimental equipment and techniques

Although all test facilities were described in detail in the above-mentioned article, a schematic diagram of the test set-up is given in figure 1. The main experiments were carried out in an air jet issuing from a 1·0 ft. diameter nozzle with an efflux velocity U of about 35 ft./s, corresponding to an exit Reynolds number of 22×10^4. For conditions far downstream from the efflux section a 0·2 ft. diameter nozzle was used instead. Evidence for axial symmetry was secured by comparing data obtained from points symmetrically located. In order to provide the reader with a proper picture of the flow under investigation, the mean velocity profiles for the region of flow establishment are presented in figure 2.

† Present address: School of Technology, S. Illinois University, Carbondale, ILL.

It was necessary to design various types of hot-wire and pressure probes. They are: (1) a triple-wire probe, for determining the one-point triple-velocity correlations. The arrangement of the wires was as follows: one wire was held normal to the direction of flow; the other two, inclined at 45° with respect to the mean-flow

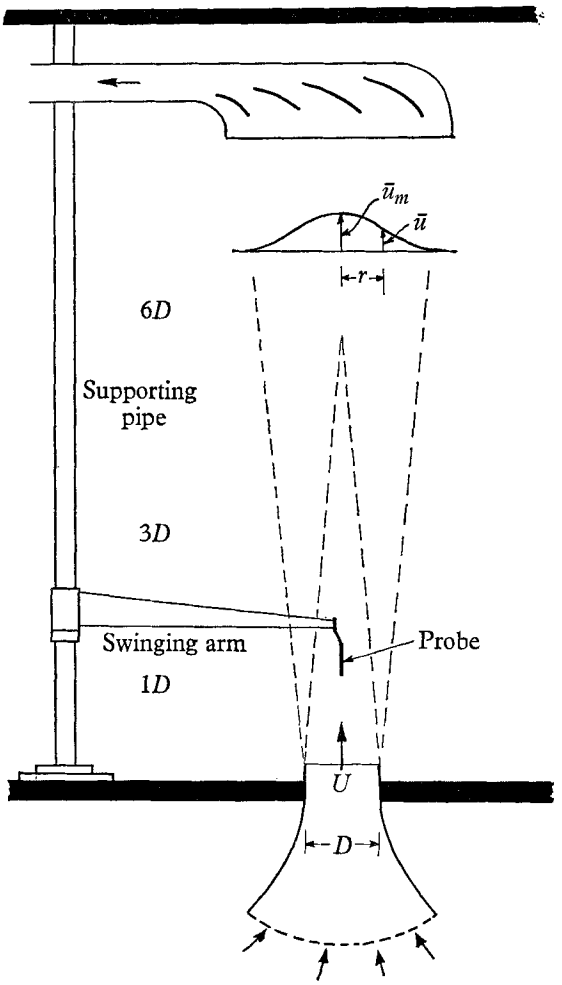

FIGURE 1. Schematic diagram of test set-up.

direction, defined with the axis of the probe two planes normal to each other. By a proper combination of their signals the anemometer yields the three fluctuating components of the velocity vector from which all the terms in the triple-velocity correlation tensor could be obtained. (2) A parallel-wire probe, designed for the measurement of the longitudinal correlation of the axial component of velocity and the longitudinal mean gradient of the axial-velocity fluctuation. One wire was held normal to the direction of flow, while the other was moved downstream. This wire was slightly displaced in the radial direction, thus avoiding any interference of its wake on the reading of the first wire. The measured correlations were assumed to be at the position of the fixed wire. (3) A parallel-wire probe,

used for measuring the radial and angular correlation of the axial component of velocity. Placed at the tips of a large compass, two parallel wires were held normal to the flow direction. By moving the legs of the compass, the wires were displaced by an equal amount in opposite directions. The measured correlations were

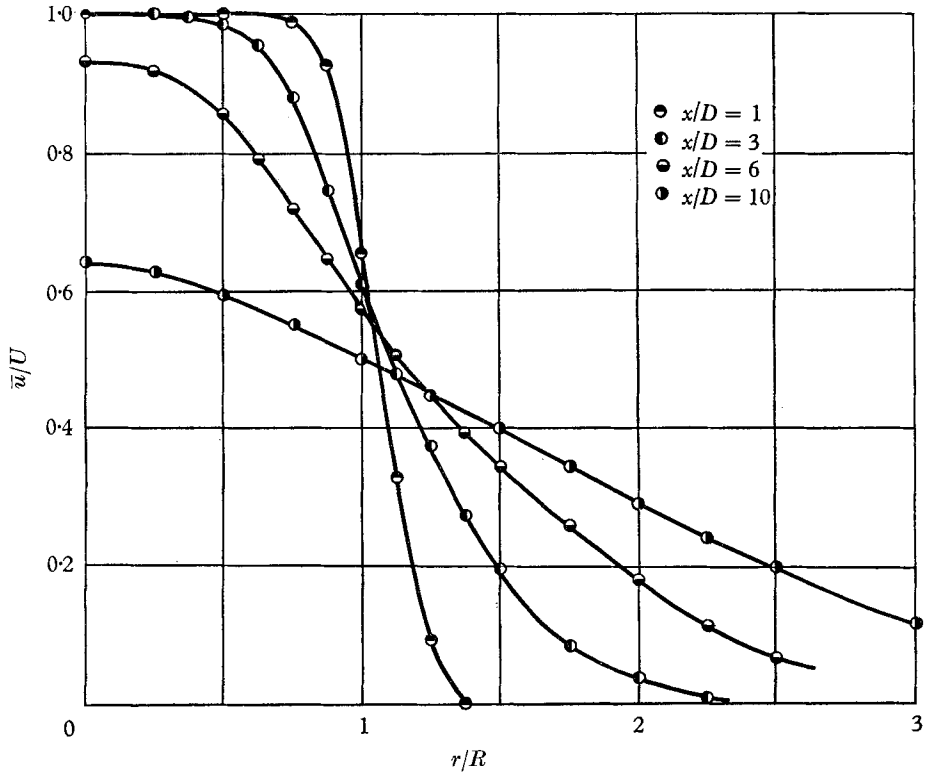

FIGURE 2. Mean axial-velocity profiles.

assumed to be at the midpoint between the two wires. For the evaluation of the spatial mean gradient of the axial-velocity fluctuations a technique introduced by Laufer (1954) was adopted. Thus, for small values of the separation vector $\bar{r}$, $\overline{u'^2} \approx \overline{u'(\bar{r})^2}$, and the spatial gradient of the axial component of turbulent velocity can be expressed as

$$\overline{\left(\frac{\partial u'}{\partial \bar{r}}\right)^2} = \lim_{r \to 0} \{\overline{[u' - u'(\bar{r})]^2}/r^2\}.$$

This was easily obtained from the experimental results of $\overline{[u' - u'(\bar{r})]^2}$ plotted against r^2.

For the measurement of the one-point pressure–velocity correlation it was necessary to obtain simultaneously the fluctuating components of both pressure and velocity. As a basis for the design of such a probe the simple hemispherical head at the end of a shaft of the same diameter was retained. However, this probe proved to be unreliable and, as a result, an indirect method has been used to determine the pressure/axial-velocity correlation term appearing in the tur-

bulence energy equation. A stagnation tube using a single 0·063 in. diameter length-expander-type ceramic located at its tip was designed for the purpose. Its construction details are shown in figure 3.

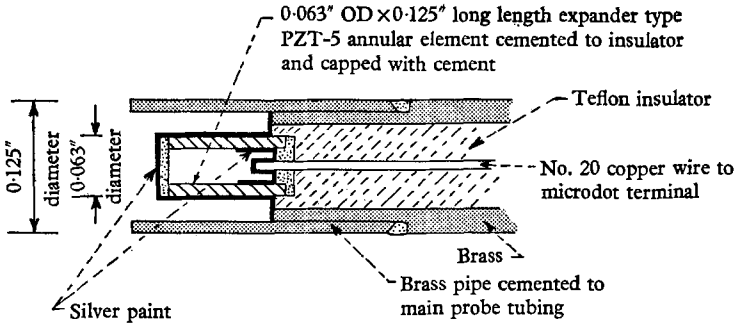

FIGURE 3. Design details of stagnation probe.

3. Evaluation and discussion of results

Macroscales of turbulence

A length scale that is representative of the mean dimensions of the eddies is defined by

$$\mathscr{L}_{\bar{r}} = \int R_{\bar{r}}\, d\bar{r},$$

where $R_{\bar{r}}$ is the normalized two-point double-velocity correlation function expressed by

$$R_{\bar{r}} = \overline{u'.u'(\bar{r})}/\overline{u'^2},$$

where $\bar{r}$ is the separation vector. During the present study the axial, radial and tangential scales of turbulence were obtained using the area under the normalized two-point double-velocity correlation function $R_{\bar{r}}$. A non-dimensional plot of $\mathscr{L}_x/D$, $\mathscr{L}_r/D$ and $\mathscr{L}_\theta/D$ against x/D for $r/R = 1$ is presented in figure 4. The axial length scale is seen to be nearly twice the radial and tangential scales.

Microscales of turbulence

In the course of this investigation the microscale of turbulence was first studied on the basis of the usual assumptions of isotropy and of undisturbed transport of turbulence characteristics over the field. The results were presented in the previous article. However, there is a considerable amount of evidence to the effect that the dissipation rate obtained by assuming isotropic conditions is not quite applicable to such anisotropic conditions. Bradbury (1965) had in fact found it 'necessary to scale the measured distribution of the viscous dissipation by a factor of nearly two in order to obtain a sensible energy balance'. Laufer (1954), on the other hand, by using a different approach found that the dissipation rate determined through the usual assumptions 'was smaller by approximately a factor of 2·5'. During the present study, Laufer's technique was adopted for the measurement of the various terms of the dissipation-rate expression. It was assumed that the mean-square derivatives with respect to a given direction

separately satisfied the isotropic relations. The results are presented in figures 5–7. They show that the dissipation length in the axial direction is considerably greater than those in the other two directions.

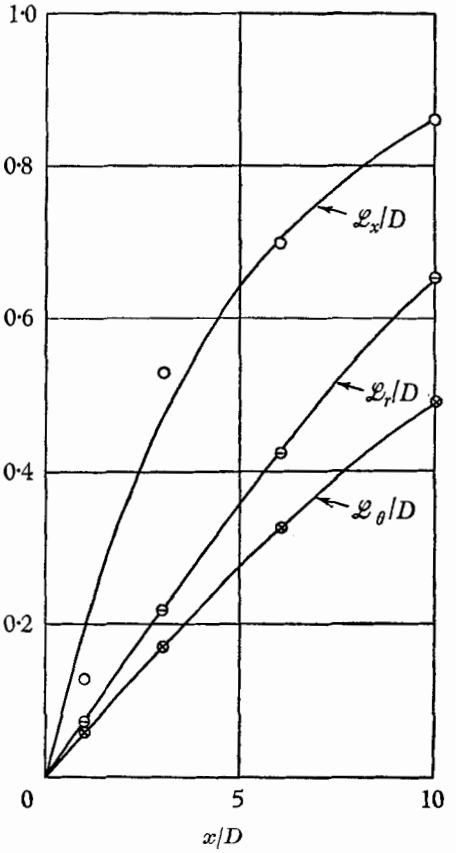

FIGURE 4. Axial, radial and tangential scales of turbulence for $r/R = 1$.

Triple-velocity correlations

The diffusion term of the turbulence energy equation consists of various one-point triple-velocity correlations ($\overline{u'^2v'}$, $\overline{v'^3}$, $\overline{v'w'^2}$, $\overline{u'^3}$, $\overline{u'v'^2}$, $\overline{u'w'^2}$). They were obtained using a triple-wire anemometer probe. The terms contributing most to the diffusion process are combined and presented in figure 8. Hot-wire measurements conducted during this study were not corrected for the effect of high turbulence intensity on hot-wire signals. The correction coefficients presented by Henkestad (1965) for the region of fully established flow of a plane jet indicate that an increase of 10–20 % in the magnitude of the Reynolds stresses would be necessary in order to correct for geometric non-linearity.

Pressure–velocity correlations

The pressure-transport term in the turbulence energy equation requires the evaluation of the one-point pressure–velocity correlations $\overline{u'p'}$ and $\overline{v'p'}$. In order to measure both correlations, a probe with a hemispherical head was first

designed and constructed. Its dynamics have already been discussed by Rouse (1954). Ceramics located behind the various piezometer holes of this hemispherical head were connected through a suitable circuitry and signals indicating u', v' or p' could easily be put through a mean-product computer to obtain $\overline{u'p'}$ or $\overline{v'p'}$. Howevei, in spite of extremely lengthy efforts aimed at improving the

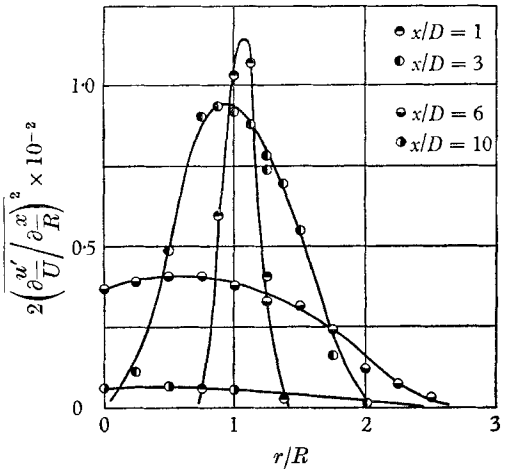

FIGURE 5. Axial gradient of the longitudinal fluctuation component.

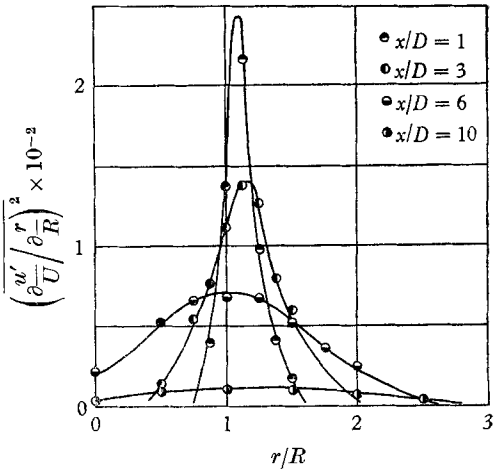

FIGURE 6. Radial gradient of the longitudinal fluctuation component.

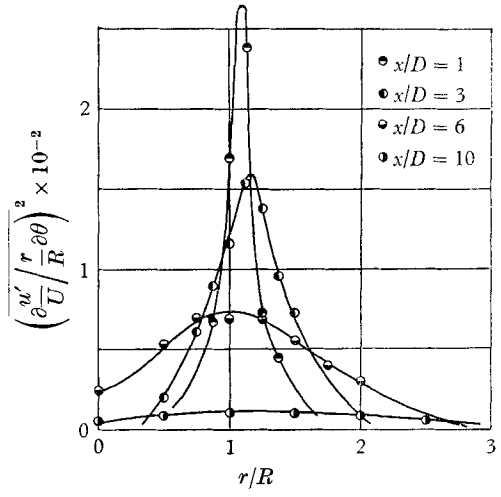

FIGURE 7. Tangential gradient of the longitudinal fluctuation component.

performance of the probe, the measurements were found to be completely unreliable. Insulating the ceramics as well as finding crystals with matching characteristics were the main obstacles. The relatively large size of the probe was a no less serious handicap. Since the integral form of the turbulence energy equation involves only $\overline{u'p'}$, an attempt was made to approximate the pressure–velocity correlation $\overline{u'p'}$ indirectly. To that effect a stagnation-pressure probe has been

constructed. The mechanics of it were presented by Ippen & Raichlen (1957) and the probe itself was used (Perkins & Eagleson 1959) in water to measure the velocity fluctuations in low-intensity turbulence. Since the ceramic transducer does not respond to average pressures, the effective pressure to which it would

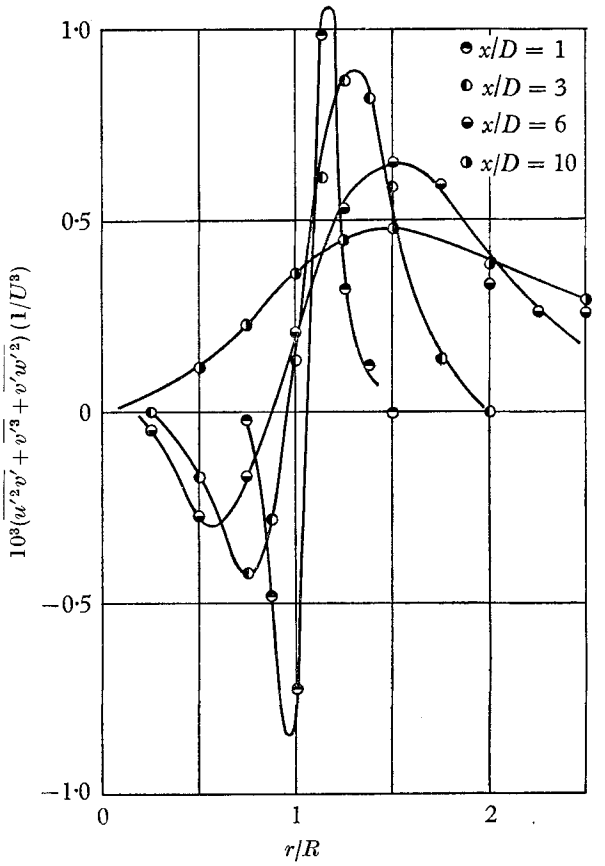

FIGURE 8. Triple-velocity-fluctuation correlations.

react is given by $p' + \rho\bar{u}u' + \frac{1}{2}\rho u'^2$. The order of magnitudes of the various terms, for the region of flow establishment of the jet, suggests that the third term can be neglected in comparison to the rest. The signal from the probe is thus reduced to $p' + \rho\bar{u}u'$. In dimensionless form, the mean square of this instantaneous signal can be written as

$$\frac{\overline{p'^2}}{(\frac{1}{2}\rho U^2)^2} + 4\frac{\bar{u}^2}{U^2}\frac{\overline{u'^2}}{U^2} + 8\frac{\bar{u}}{U}\frac{\overline{u'p'}}{\rho U^3}.$$

Since the mean-velocity field as well as the velocities and pressures associated with turbulence were determined previously, the pressure–velocity correlation term $\overline{u'p'}/\rho U^3$ could be evaluated by subtraction. It must be pointed out at the outset that such a technique cannot lead to a direct and accurate measurement of the term under study. But it can give valuable information about its sign and its order of magnitude. The computed values of $\overline{u'p'}/\rho U^3$ are given in figure 9. It

is apparent that near the nozzle the high-frequency fluctuations were not properly recorded by the probe. Turbulence-intensity and shear measurements carried out in the same region had also indicated a similar deficiency on the part of the hot-wire equipment. It was therefore reasonable to increase the magnitude of the

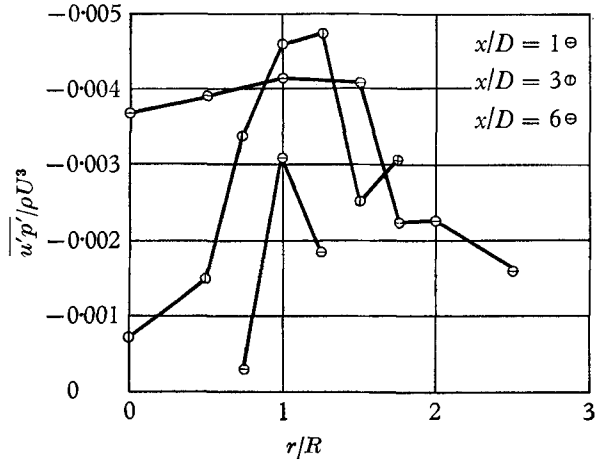

FIGURE 9. Computed values of pressure–velocity correlation term.

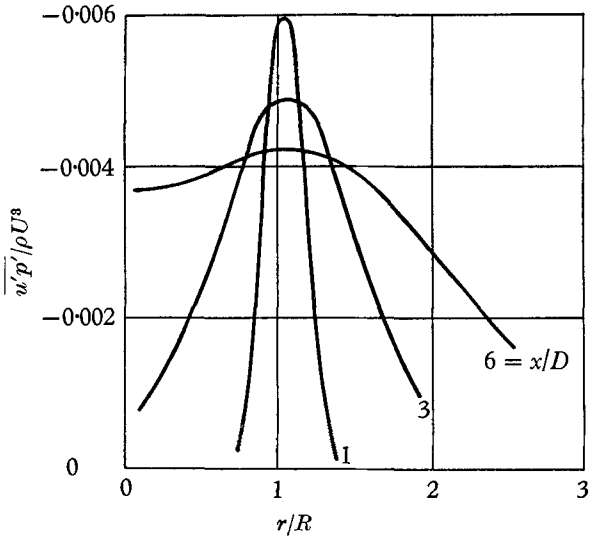

FIGURE 10. Adjusted curves of pressure–velocity correlation term.

values measured in the vicinity of the nozzle. The criteria used for the consistency of the data along the shear layer was that of obtaining a continuously decreasing function when they were plotted against distances measured from the lip of the nozzle. The final curves as presented in figure 10 were later used for evaluating the axial gradient of the pressure–velocity correlation term $\overline{u'p'}/\rho U^3$.

Turbulence energy analysis

The differential and integral forms of the turbulence energy relationship are (Rouse 1960):

$$\underbrace{\left[\frac{\overline{u'v'}}{U^2}\left(\frac{\partial}{\partial(r/R)}\frac{\bar{u}}{U}+\frac{\partial}{\partial(x/R)}\frac{\bar{v}}{U}\right)+\frac{1}{2}\frac{\overline{u'^2}}{U^2}\frac{\partial}{\partial(x/R)}\frac{\bar{u}}{U}\right]}_{\text{Production}}+\underbrace{\left[\frac{1}{2}\frac{\bar{u}}{U}\frac{\partial}{\partial(x/R)}\frac{\overline{V'^2}}{U^2}+\frac{\bar{v}}{U}\frac{\partial}{\partial(r/R)}\frac{\overline{V'^2}}{U^2}\right]}_{\text{Convection}}$$

$$+\underbrace{\left[\frac{\partial}{\partial(x/R)}\frac{\overline{u'p'}}{\rho U^3}+\frac{1}{r/R}\frac{\partial}{\partial(r/R)}\frac{r}{R}\frac{\overline{v'p'}}{\rho U^3}\right]}_{\text{Pressure-transport}}$$

$$+\frac{1}{2}\underbrace{\left[\frac{\partial}{\partial(x/R)}\left(\frac{\overline{u'^3}}{U^3}+\frac{\overline{u'v'^2}}{U^3}+\frac{\overline{u'w'^2}}{U^3}\right)+\frac{\partial}{\partial(r/R)}\left(\frac{\overline{u'^2v'}}{U^3}+\frac{\overline{v'^3}}{U^3}+\frac{\overline{v'w'^2}}{U^3}\right)+\frac{1}{r/R}\left(\frac{\overline{u'^2v'}}{U^3}+\frac{\overline{v'^3}}{U^3}+\frac{\overline{v'w'^2}}{U^3}\right)\right]}_{\text{Diffusion}}$$

$$+\underbrace{\frac{1}{R_R}\frac{R}{U^2}\left[\overline{\left(\frac{\partial u'}{\partial x}\right)^2}+\overline{\left(\frac{\partial v'}{\partial x}\right)^2}+\overline{\left(\frac{\partial w'}{\partial x}\right)^2}+\overline{\left(\frac{\partial u'}{\partial r}\right)^2}+\overline{\left(\frac{\partial v'}{\partial r}\right)^2}+\overline{\left(\frac{\partial w'}{\partial r}\right)^2}+\overline{\left(\frac{\partial u'}{r\partial\theta}\right)^2}+\overline{\left(\frac{\partial v'}{r\partial\theta}\right)^2}+\overline{\left(\frac{\partial w'}{r\partial\theta}\right)^2}\right]}_{\text{Dissipation: }\phi}=0, \tag{1}$$

and

$$\underbrace{4\int\int\left[\frac{\overline{u'v'}}{U^2}\left(\frac{\partial}{\partial(r/R)}\frac{\bar{u}}{U}+\frac{\partial}{\partial(x/R)}\frac{\bar{v}}{U}\right)+\frac{1}{2}\frac{\overline{u'^2}}{U^2}\frac{\partial}{\partial(x/R)}\frac{\bar{u}}{U}\right]\frac{r}{R}d\frac{r}{R}d\frac{x}{R}}_{\text{Production}}$$

$$+\underbrace{2\int\frac{\bar{u}}{U}\frac{\overline{V'^2}}{U^2}\frac{r}{R}d\frac{r}{R}}_{\text{Convection}}+\underbrace{2\int\frac{\overline{u'V'^2}}{U^3}\frac{r}{R}d\frac{r}{R}}_{\text{Diffusion}}+\underbrace{4\int\frac{\overline{u'p'}}{\rho U^3}\frac{r}{R}d\frac{r}{R}}_{\text{Pressure-transport}}+\underbrace{4\int\int(\phi)\frac{r}{R}d\frac{r}{R}d\frac{x}{R}}_{\text{Dissipation}}=0. \tag{2}$$

For $x/D = 6$, the pressure-transport term of the integral form of turbulence energy equation has been evaluated from collected data and plotted together with the diffusion term. For $x/D = 10$ and 20 it was obtained by difference and plotted as a closing entry. The pressure-transport term of the differential form of the same equation could only be obtained by difference, since it involved $\overline{v'p'}$ as well. The results are shown in figures 11–17. They indicate that, for the region of flow establishment, all energy transformations take place within the mixing zone. As it would be expected, along the shear layer production is extremely high and is balanced by diffusion and dissipation. However, at the edges of the mixing zone, convection by the mean flow and diffusion by turbulence and pressure assume a role opposite to the one observed along the free-shear layer, and as a result their contributions to the energy balance are reversed. Considering the self-preserving nature of the mixing layer in the region near the nozzle, the turbulence energy balance for $x/D = 3$ after a suitable transformation can be compared with the early work of Liepmann & Laufer (1947) in a two-dimensional free mixing layer.† As it can be seen in figure 14 the results for the round jet correspond quite closely to the behaviour of the two-dimensional free mixing layer.

† This comparison was suggested by a referee.

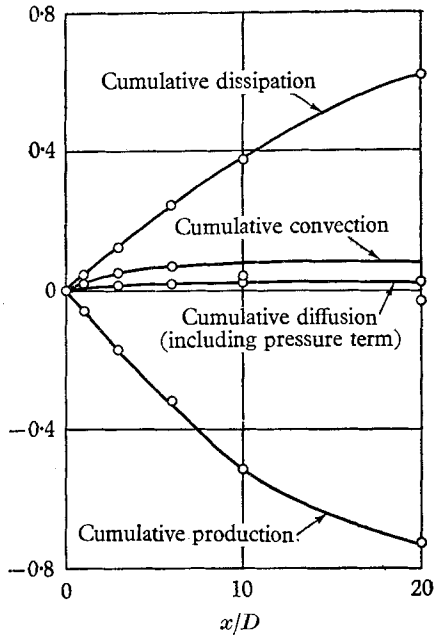

FIGURE 11. Turbulence energy analysis—integral form.

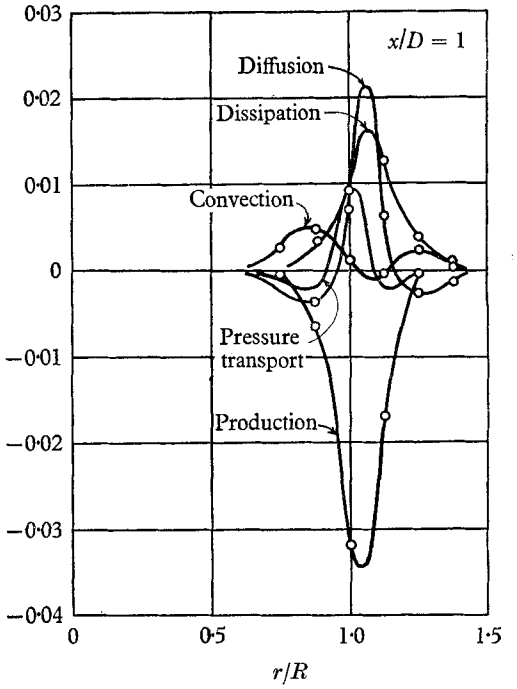

FIGURE 12. Turbulence energy analysis at $x/D = 1$.

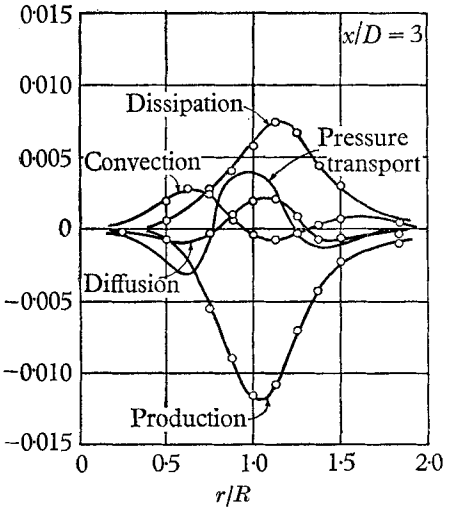

FIGURE 13 Turbulence energy analysis at $x/D = 3$.

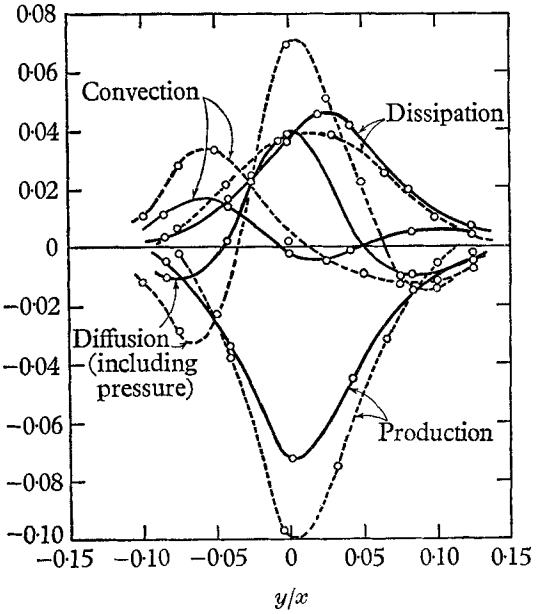

FIGURE 14. Comparison of the energy balance at $x/D = 3$ with the results of Liepmann & Laufer (1947) for a free mixing layer. ——, Liepmann & Laufer.

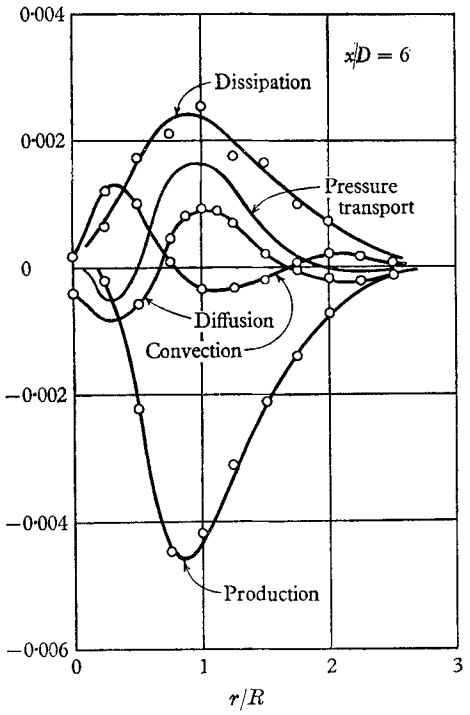

FIGURE 15. Turbulence energy analysis at $x/D = 6$.

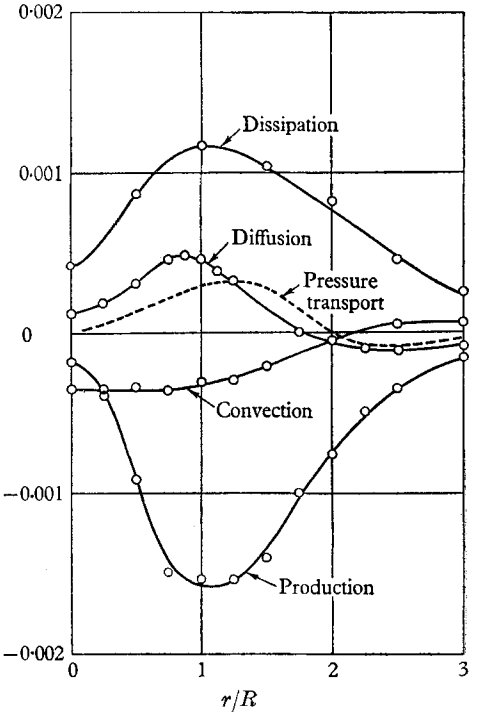

FIGURE 16. Turbulence energy analysis at $x/D = 10$.

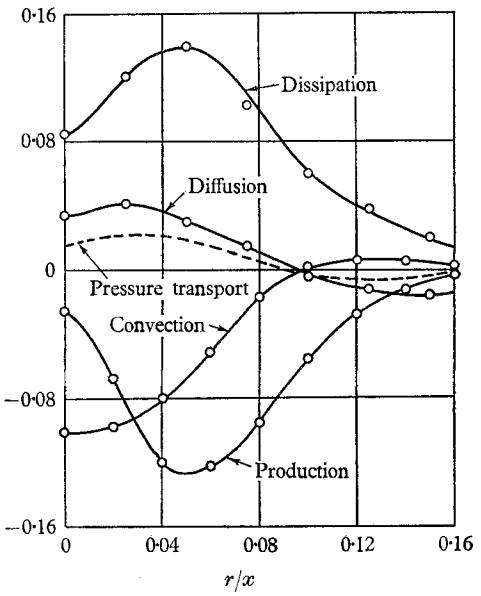

FIGURE 17. Turbulence energy analysis—similarity zone.

In the region of established flow, the effect of the central core disappears completely and the overall pattern of the lateral distribution of the various terms is quite similar to that given by Townsend (1956) for the wake flow, by Bradbury (1965) and Henkestad (1965) for the plane jet.

4. Conclusion

Measurements of mean-flow and turbulence characteristics made in the region of flow establishment of a turbulent jet indicate a very high level of turbulence along the shearing surface, a strongly intermittent character in the regions adjacent to the non-turbulent flow, and an axial length scale nearly twice as large as the radial and tangential ones. The approximate values obtained for the one-point pressure/axial-velocity correlation indicate a negative correlation between the instantaneous fluctuations of pressure and axial velocity.

An analysis of the turbulence energy equation indicated that: (1) the two most significant contributions to the turbulent energy balance in the mixing region are the production and the dissipation terms; (2) the contributions of turbulence-diffusion and pressure-transport terms to the turbulence energy balance appear to be not only of similar magnitude but also almost everywhere in the same direction.

The author would like to thank Prof. Hunter Rouse and the staff of the Iowa Institute of Hydraulic Research of The University of Iowa for their help and encouragement during the course of this research. Thanks are also due to the referees for their critical review of the manuscript. The project as a whole was supported by the Office of Naval Research under Contract Nonr 1509(03) with the Institute.

REFERENCES

BRADBURY, L. J. S. 1965 The structure of a self-preserving turbulent plane jet. *J. Fluid Mech.* **23**, 31.

HENKESTAD, G. 1965 Hot-wire measurements in a plane turbulent jet. *A.S.M.E. J. Applied Mech.* **32**, 721.

IPPEN, A. T. & RAICHLEN, F. 1957 Turbulence in civil engineering: measurements in free surface streams. *Proc. A.S.C.E.* no. 83, paper no. 1392.

LAUFER, J. 1954 The structure of turbulence in fully developed pipe flow. *NACA Rept.* no. 1174.

LIEPMANN, H. W. & LAUFER, J. 1947 Investigations of free turbulent mixing. *NACA TN*, no. 1257.

PERKINS, F. E. & EAGLESON, P. S. 1959 The development of a total head tube for high frequency pressure fluctuations in water. *M.I.T. Hydrodynamics Lab. Tech. Note*, no. 5.

ROUSE, H. 1954 Measurements of velocity and pressure fluctuations in the turbulent flow of air and water. *Extrait des Mémoires sur la Mécanique des Fluides offerts à M. D. Riabouchinsky a l'occasion de son Jubilé Scientifique.* Publ. Sci. et Tech. du Ministère de l'Air.

ROUSE, H. 1960 Distribution of energy in regions of separation. *La Houille Blanche*, nos. 3 and 4.

SAMI, S., CARMODY, T. & ROUSE, H. 1967 Jet diffusion in the region of flow establishment. *J. Fluid Mech.* **27**, 231.

TOWNSEND, A. A. 1956 *The Structure of Turbulent Shear Flow.* Cambridge University Press.